PHYSICAL REVIEW B VOLUME 27, NUMBER 11 1 JUNE 1983

Pattern formation in directional solidification

Michel Kerszberg
Department of Physics, Harvard University, Cambridge, Massachusetts 02138
(Received 17 January 1983)

The one-sided model for a nearly planar solidification front advancing at steady velocity is studied. The model neglects impurity diffusion in the solid; the interface is stabilized by the imposition of a thermal gradient. The front, located at $z_s = z_s(x,y)$, is described by the coefficients $\epsilon_{\vec{k}}$ of the Fourier expansion for z_s, and equations of motion $\dot{\epsilon}_{\vec{k}} = f_{\vec{k}}(\{\epsilon\})$ are derived in the approximation where the velocity $\vec{v}$ of the interface is small. The functions $f_{\vec{k}}$ are expressed as infinite polynomials in the $\{\epsilon\}$. Stationary solutions $f_{\vec{k}} = 0$ are sought with the help of a consistent truncation scheme. Truncations which involve keeping terms of up to fifth order in $\epsilon_{\vec{k}}$ are used. Stationary profiles for both one- and two-dimensional fronts are obtained numerically, whose features are in reasonable agreement with experimental observations. In particular, the one-dimensional solutions exhibit a relatively well-developed cellular structure; this is in contrast with what happens in more conventional analyses, where higher-order nonlinearities are not accounted for. The two-dimensional stationary interfaces are of various types, displaying twofold or sixfold symmetry. It appears to be the first time that calculations of two-dimensional structures are reported.

I. INTRODUCTION

The various phenomena displayed by systems driven far away from thermodynamic equilibrium have often attracted the interest of physicists. Attention, however, has tended to focus mainly upon reaction-diffusion problems,[1,2] thermoconvective systems such as Rayleigh-Bénard ones,[3–7] or those involving the Couette-Taylor roll pattern.[8–11] Analysis of these problems has often proved too complicated, thus justifying the recourse to simplified models, chemical[2,12] or other.[13] This relative specialization tends to obscure the fact that the phenomena themselves are extraordinarily widespread. For instance, the general interrelation between nonequilibrium growth mechanisms and form, as observed in nature organic and inorganic, was recognized long ago.[14] In this work we report progress in understanding a particular nonequilibrium crystal growth problem, that of directional solidification, which affords a beautiful and relatively simple example of interaction linking growth and shape.[15] In spite of a long-standing interest in the varied forms exhibited by snowflakes,[16,17] it is only very recently that theorists have begun serious efforts aimed at understanding the so-called "morphological" aspects of crystal growth.[18–24]

It may at first appear mysterious why the surface of a growing crystal should not remain macroscopically as flat as possible. This would seem to be the inevitable effect of surface tension. As Mullins and Sekerka have pointed out,[19] however, a powerful destabilizing mechanism exists. As we shall see, the equations governing diffusion-controlled crystal growth are closely related to the Laplace equation of, say, electrostatics; just as the electric field is increased at the tip of a lightning rod, thus diverting electric currents toward it, the slightest bulge on a growing crystal surface increases the diffusion-driving gradient there, which leads to faster growth and further perturbation of the initial interface. Actually, this effect is so strong as to render the growth of a flat crystal face from supersaturated solution *always* unstable, unless an additional stabilizing force, such as a thermal gradient, is present. The planar interface then appears to be stable, provided the dimensionless growth velocity, which plays the role of the driving parameter, lies below some threshold. Beyond the threshold, a variety of stationary structures, all of which can be described as "cellular," are observed.[25,26] The reader may get some idea of their main characteristics by glancing at Figs. 1 and 2; these figures exhibit some of the results of our calculations and they agree quite well with known experimental facts. In a typical directional solidification experiment,[26] a thin sample of CBr_4 contained between microscope slides moves at a constant velocity $-V_z$ ($V_z > 0$) between a hot plate and a cold plate located, respectively, at $z_0 > 0$ and $-z_0$. In this way two fronts are created which ad-

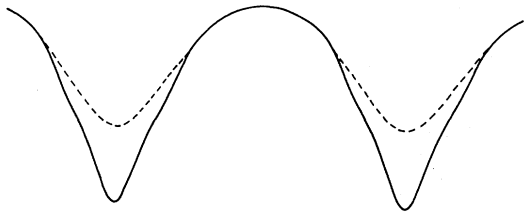

FIG. 1. Stationary one-dimensional cellular interface structure, as calculated from truncated Eq. (28), with $\rho=10^2$, $\nu=1.15$, and $\kappa_0=0.14$. The liquid phase is on the top of the picture. The dashed line denotes the solution when Eq. (28) is truncated at order $n=3$ (see text). The amplitude of the higher harmonics $i\kappa_0$ is then not determined with good accuracy. The solid line illustrates the fourth-order ($n=4$) solution, which compares rather well with some experimental results (Refs. 26 and 37). (The vertical and horizontal scales are the same.)

vance with respect to the sample: The solid melts at one front and resolidifies at the other. Here we shall consider only what happens at the solidification front. For low enough V_z, this front is *planar*; however, above a threshold velocity[27] a one-dimensional structure appears, characterized by sharp and regularly spaced cusps pointing in the $z<0$ direction[18,26] (Fig. 1). The spacing of the cusps is typically of the order of 50 μm. Further away from threshold, the structure becomes dendritic: Growth takes place in a complicated, "treelike" fashion; we shall not attempt here to analyze this regime.

Compared with other nonequilibrium pattern formation problems, the structures seen in directional solidification seem to present some interesting features. First, as we have seen, in properly arranged experiments phenomena are essentially one dimensional; at least they can be understood in a relatively satisfactory way using a purely one-dimensional analysis. This is a welcome simplification for the theorist. Two-dimensional interfaces, on the other hand, exhibit a wider variety of stationary states than, say, Rayleigh-Bénard systems [see Figs. 2(a) and 2(b)]. Finally, it is worth noting that because the cellular spacing is typically so small, the approximation that the system is infinite is certainly a far less dangerous one in this context than it has proved to be in other nonequilibrium systems.[5] As against all this, the strength of the instability mechanism appears such that the structures seen are never as simple as pure Rayleigh-Bénard rolls, but

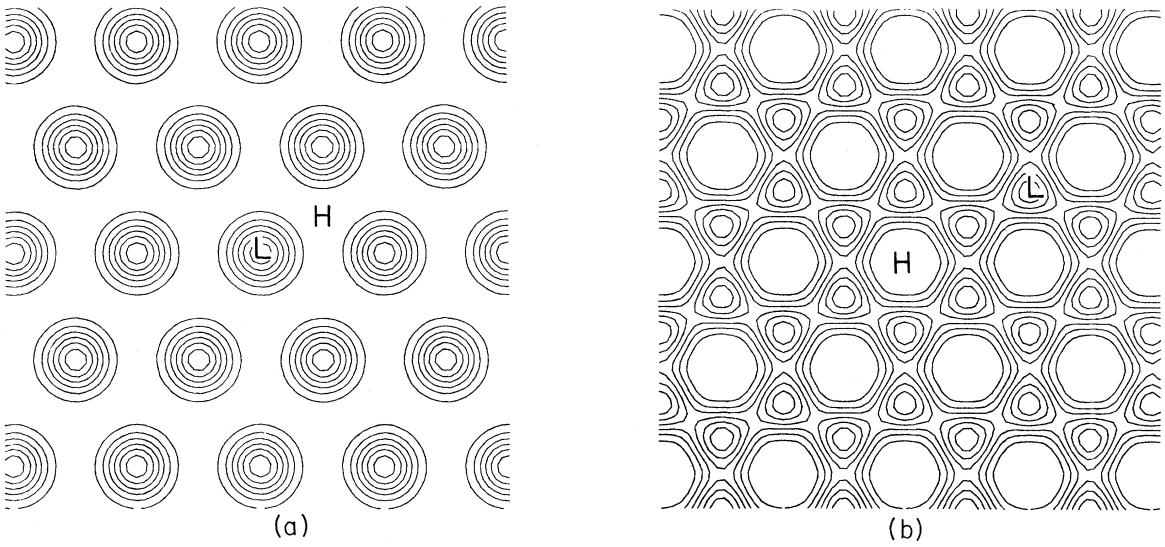

FIG. 2. Two-dimensional interface structures, computed as stationary solutions of Eq. (28), truncated to third order. The modes included in the analysis (see text) are indicated in Fig. 4. The solutions are represented as contour plots; the solidification front should be pictured as advancing out of the page, with the letter H indicating a high, or warm point, while L denotes a low, or cold point on the surface. (a) This solution can be described as a triangular array of "pits." (b) In this configuration, the interface is covered by a hexagonal array of "grooves," which meet at the lowest points. Solutions (2a) and (2b) are both for $\nu=1.105$, $\rho=10^2$, and $\kappa_1=(0.15,0)$. There is a third possible solution with the same parameter values, i.e., one where the one-dimensional solution (such as shown in Fig. 1) is seen as the result of cutting an array of infinite straight grooves extending perpendicularly to the page. Nothing is known at present as to the relative stability of these three solutions.

result rather from the nonlinear interaction of a large number of modes. As we shall see, this apparently requires that the analysis of these effects sometimes take account of terms of unusually high order, even not very far from threshold; only then do qualitatively satisfying patterns emerge from the calculations.

In this paper we set up equations of motion for a relatively realistic model of solidification; we show how a cellular structure, exhibiting the nonlinearity mentioned above, is obtained from the steady solution of the equations. In the one-dimensional case, we do this with much attention to the precision of the calculations; this leads us to consider the effect of terms of fourth and even fifth order in the deviations from flatness. The results mark a considerable improvement over previous analyses.[28] To our knowledge, this is the first time that such a detailed semiquantitative understanding of the cellular pattern is obtained without the use of any *ad hoc* assumption. In the two-dimensional case, we limit ourselves to a simpler third-order analysis; our results already display, however, the basic features seen in the experiments.[25] As far as we know, no calculation of two-dimensional interface structures has been reported previously.

The remainder of this paper is organized as follows. In Sec. II we describe in detail the physical system under consideration, and discuss the assumptions that lie behind the model we have adopted. In Sec. III we outline the derivation of the fundamental "equations of motion" for this model. Some of the detailed calculations are postponed until Appendix A, while the equations themselves are summarized in Appendix B. Sections IV and V are devoted, respectively, to a discussion of the one- and two-dimensional stationary (numerical) solutions of the equations. Finally, we present in Sec. VI some remarks and general conclusions.

II. THE MODEL

We shall use the "one-sided" model[18,20] for the solidification of a binary mixture; in this model, diffusion of the impurity is neglected on the solid side of the interface. This is certainly an excellent approximation in the systems of interest. It should be noted that the techniques we shall use do not preclude the possibility of relaxing this approximation; but we do not expect that this would unravel qualitatively new phenomena. We shall also assume that the temperature field is essentially as imposed from the outside. This will be accurate provided the latent heat of solidification, which is released at the interface, is relatively small while the thermal diffusivities are much larger than the chemical ones; we can then write

$$T(z)=T_0+Gz \quad , \tag{1}$$

with $z=0$ the conventional position of the solidification front, to be determined later. The diffusion of the impurity is controlled by a Fick equation; with c the concentration, the equation reads

$$\frac{\partial c}{\partial t}=D\nabla^2 c+V_z\frac{\partial c}{\partial z} \quad , \tag{2a}$$

where due respect has been paid to the fact that the sample is moving in the z direction, as described in the Introduction. We can rewrite Eq. (2a) as an equation for the chemical potential μ: One has approximately

$$\mu-\mu_{\rm eq}=\left.\frac{\partial\mu}{\partial c}\right|_{\rm eq}(c-c_{\rm eq}) \quad , \tag{2b}$$

where the subscript eq refers to equilibrium values on the liquid side of a flat interface at temperature T_0 (liquidus line): we shall take from now on $\mu_{\rm eq}=0$. We thus have

$$\frac{\partial\mu}{\partial t}=D\nabla^2\mu+V_z\frac{\partial\mu}{\partial z} \quad . \tag{2c}$$

We now determine the boundary conditions that must accompany this equation. Let us first note that the establishment of a steady state clearly requires that the concentration c_∞ far away[29] from the interface be the same on both sides. Since the sample is initially solid, it is thus natural to fix T_0 as the temperature where, on the *solidus* line, the concentration $c'_{\rm eq}$ is equal to c_∞. Now since the miscibility gap $c_{\rm eq}-c'_{\rm eq}=\Delta C>0$, our conventions, together with (2b), imply that

$$\begin{aligned}\mu_{z\to\infty}&=A(c_\infty-c_{\rm eq})\\&=-A\Delta C<0 \quad ,\end{aligned} \tag{3a}$$

where $A=\text{const}=\partial\mu/\partial c$. Hereafter, we assume a normalization $\mu\to\mu/(A\Delta C)$ such that

$$\mu_{z\to\infty}=-1 \quad . \tag{3b}$$

This gives the boundary condition at infinity. Equations (2c) and (3b) are linear, but this is not the case of the boundary condition on the interface, which we now consider. In doing so we assume that, at the interface itself, "local equilibrium" prevails, i.e., except for the presence of the impurity flux, the interface behaves exactly as an equilibrium one. Several phenomena may be responsible for departures from this situation; they are mainly the following.

(a) "Attachment kinetics": If we regard the "loosening" of impurity atoms, or alternatively, the

"attachment" of solvent atoms at the surface, as a chemical reaction, then the kinetics of this reaction may in fact control the solid's growth.[30] We shall assume such reactions operate at their equilibrium point.

(b) Surface diffusion: The diffusion of surface atoms between sites on the surface may contribute significantly[31] to the redistribution of impurity. We shall neglect surface diffusion.

Note that interface nonequilibrium is certainly a major factor in several circumstances, such as the fast growth (several m/s) which occurs in laser annealing.[32] In our context, local equilibrium implies that, with the flat interface located at $z=0$, the chemical potential there can be assumed to be $\mu_s=0$ on both sides; this may change due to deviation from flatness—which gives rise to the well-known Gibbs-Thomson curvature effect[33]—and to temperature variations, which stem from the interface moving in the temperature field (1). Thus one has

$$\mu_s=-d\Gamma-\alpha z_s \quad , \tag{4}$$

where d and α are coefficients proportional, respectively, to surface tension and to the temperature gradient G (expressions for d and α in terms of thermodynamic quantities are given in Ref. 18), z_s is the interface coordinate, while Γ is the mean curvature[34]

$$\Gamma(x,y)=\vec{\nabla}\cdot\left[\frac{\vec{\nabla}z_s(x,y)}{[1+(\vec{\nabla}z_s)^2]^{1/2}}\right] \quad . \tag{5}$$

Note that in (4), we have neglected the anisotropy of surface tension. This amounts to the assumption that the interface is microscopically very rough.[35] Even so, because of the form of (5), the differential problem to be solved, i.e., (2c) together with (3b) and (4) imposed on z_s, is strongly nonlinear. This nonlinearity will ultimately show up in the equations of motion for the interface, which we now derive.

III. EQUATIONS OF MOTION

We now write the equation of the interface as

$$z_s(\vec{x})=\sum_{\vec{k}}\epsilon_{\vec{k}}\epsilon_{\vec{k}}e^{i\vec{k}\cdot\vec{x}} \quad , \tag{6}$$

with $\vec{k}=(k_x,k_y)$ a general wave vector, and $\vec{x}=(x,y)$ the coordinates in the plane orthogonal to z. Our goal is to find the equations of motion $\dot{\epsilon}_{\vec{k}}=f(\{\epsilon\})$. The procedure we must follow is simple but extremely tedious. Assuming some values for the $\epsilon_{\vec{k}}$'s we (a) solve (2c) together with (3b) and (4); (b) find, from the solution μ, the impurity flux away from the interface, $\vec{j}$, proportional to the gradient of μ, and hence the growth rate $\Delta C\vec{v}\cdot\vec{n}=\vec{j}\cdot\vec{n}$, where $\vec{n}$ is the exterior unit normal to the interface. From $\vec{v}\cdot\vec{n}$ we derive an expression for $\dot{\epsilon}_{\vec{k}}$. Note that we take ΔC to be independent of temperature and curvature; lifting this restriction can have important effects, which we shall discuss in Sec. VI. Clearly, the major step in the above program consists in solving Eq. (2c); before proceeding, we shall introduce an important additional approximation. Let us stress that the approximation is not essential in principle and that the techniques we shall use allow for its removal, but this is at the price of even more lengthy calculations. To keep these within limit, we shall assume[19] that the interface moves rather slowly, so that Eq. (2c) can effectively be written

$$D\nabla^2\mu+V_z\frac{\partial\mu}{\partial z}=0 \quad . \tag{2c'}$$

This so-called "quasistationary approximation" has been discussed previously in the literature.[18,19] We shall later state the condition under which it is valid; in practice, the condition is usually satisfied.

Even (2c'), however, is not easy to solve when the interface is not flat. The difficulty of the question may appear to the reader if we note that, although the problem of solving a partial differential equation with boundary conditions imposed on a slightly deformed contour (6) is certainly a generic one in mathematical physics, a simple and systematic method of solution has been published[36] only in 1973. The idea is, basically, to write successive differential problems for the partial derivatives $\partial^n\mu/\partial\epsilon_{\vec{k}_1}\cdots\partial\epsilon_{\vec{k}_n}$, and solve these to zeroth order in the $\epsilon_{\vec{k}}$'s. The partial derivatives then generate the Taylor expansion for μ. In order to illustrate the principle of the solution, let us consider for simplicity only one mode $\epsilon_{\vec{k}}=\epsilon$. Let us concentrate on the variation of μ with ϵ; if we denote $\partial\mu/\partial\epsilon\equiv\mu_\epsilon$, we have, from (2c'):

$$D\nabla^2\mu_\epsilon+V_z\frac{\partial\mu_\epsilon}{\partial z}=0 \quad . \tag{7}$$

In finding the boundary condition to be associated with (7), we must not forget that varying ϵ by $\delta\epsilon$ leads to a motion of the interface

$$\delta z_s=\delta\epsilon\, e^{i\vec{k}\cdot\vec{x}} \quad , \tag{8}$$

so that

$$\frac{\partial\mu_s}{\partial\epsilon}\equiv(\mu_s)_\epsilon=(\mu_\epsilon)_s+(\nabla_z\mu)_s e^{i\vec{k}\cdot\vec{x}} \quad , \tag{9}$$

where $(\mu_\epsilon)_s$ denotes the partial derivative μ_ϵ evaluated on the surface. We can thus write the boundary

condition for (7):

$$(\mu_\epsilon)_s=(\mu_s)_\epsilon-(\nabla_z\mu)_s e^{i\vec{k}\cdot\vec{x}} \ , \tag{10}$$

in which $(\mu_s)_\epsilon$ can be computed explicitly from (4). It would not seem that we have accomplished much, since μ appears in (10) and is itself unknown. Furthermore, if we could not solve the original problem for μ, the new one appears just as difficult. The point, however, is that we want to solve (7) with (10) only to *zeroth* order in ϵ. In particular, the domain to be considered is that formed of the liquid phase bounded by the unperturbed, or *flat* interface, and the function μ required in (10) is just the solution when $\epsilon=0$, which is easy to find. When μ_ϵ is thus determined everywhere, we may proceed and write

$$D\nabla^2\mu_{\epsilon\epsilon}+V_z\frac{\partial\mu_{\epsilon\epsilon}}{\partial z}=0 \ , \tag{11}$$

with boundary condition

$$(\mu_{\epsilon\epsilon})_s=(\mu_s)_{\epsilon\epsilon}-2\nabla_z\mu_\epsilon e^{i\vec{k}\cdot\vec{x}}-\frac{\partial^2\mu}{\partial z^2}e^{2i\vec{k}\cdot\vec{x}} \ . \tag{12}$$

Again, the first term on the right-hand side of (12), $(\mu_s)_{\epsilon\epsilon}$, is "easily" computed from Eq. (4), while knowledge of μ to first order in ϵ is enough to obtain the $\nabla_z\mu_\epsilon$ and $\partial^2\mu/\partial z^2$ terms to zeroth order. We can thus establish successively all the derivatives $(\partial\mu/\partial\epsilon)_{\epsilon=0}$, $(\partial^2\mu/\partial\epsilon^2)_{\epsilon=0}$, etc., and this allows us to write

$$\mu=\mu\,|_{\epsilon=0}+\left.\frac{\partial\mu}{\partial\epsilon}\right|_{\epsilon=0}\epsilon+\frac{1}{2}\left.\frac{\partial^2\mu}{\partial\epsilon^2}\right|_{\epsilon=0}\epsilon^2+\cdots \ , \tag{13}$$

thus completing the solution. It is easy to see that the generalization to more than one $\epsilon_{\vec{k}}$ is straightforward. Note that the technique is very general, and it is only the length of the calculations which has prevented us from considering, say, the full time-dependent equation (2c), or the effect of diffusion in the solid.

We now display some of the explicit computations. We shall need the expression of the mean curvature Γ as a function of the ϵ's:

$$\Gamma=\sum_{\vec{k}}e^{i\vec{k}\cdot\vec{x}}\sum_{\vec{k}'}\vec{k}\cdot\vec{k}'\epsilon_{\vec{k}'}\sum_{n=0}^{\infty}\frac{(-1)^n[(2n-1)!!]}{2^n n!}\prod_{\substack{\vec{K}_1,\ldots,\vec{K}_n\\ \sum_j\vec{K}_j=\vec{k}-\vec{k}'}}\left[\sum_{\vec{k}''}\vec{k}''\cdot(\vec{K}_i-\vec{k}'')\epsilon_{\vec{k}''}\epsilon_{\vec{K}_i-\vec{k}''}\right] \ , \tag{14}$$

and the solution of Eqs. (2c'), (3b), (4), and (5) when $\epsilon=0$, which is

$$\mu^{(0)}=-1+e^{-q_0 z} \tag{15}$$

with $q_0=V_z/D$. We describe here the calculation up to second order in ϵ, while a discussion of higher-order terms appears in Appendix A. Of course, in writing the solution as a series in ϵ, one hopes that some "low"-order approximation will afford a good precision; this question will be examined in Sec. IV.

A. First order

We have from (15), $\nabla_z\mu(z=0)=-q_0$, while from (4), $(\mu_s)_\epsilon$, calculated for $\epsilon=0$, is $(-dk^2-\alpha)e^{i\vec{k}\cdot\vec{x}}$; thus from Eq. (10),

$$\left.\frac{\partial\mu}{\partial\epsilon_{\vec{k}}}\right|_{\epsilon_{\vec{k}}=0,\ z=0}=-e^{i\vec{k}\cdot\vec{x}}(dk^2+\alpha-q_0) \tag{16}$$

and (7) yields

$$\left.\frac{\partial\mu(x,y,z)}{\partial\epsilon_{\vec{k}}}\right|_{\epsilon=0,\ \vec{k}=0}=-(dk^2+\alpha-q_0)e^{i\vec{k}\cdot\vec{x}}e^{-q(k)z} \ , \tag{17}$$

where $q(k)=q_0/2+(q_0^2/4+k^2)^{1/2}$. Finally, the first-order contribution to μ is

$$\mu^{(1)}=-\sum_{\vec{k}}\epsilon_{\vec{k}}(dk^2+\alpha-q_0)e^{i\vec{k}\cdot\vec{x}}e^{-q(k)z} \ . \tag{18}$$

B. Second order

We note first that, from (4) and (14), one has $(\mu_s)_{\epsilon_{\vec{k}_1}\epsilon_{\vec{k}_2}}=0$; thus Eq. (12) yields

$$(\mu_{\epsilon_{\vec{k}_1}\epsilon_{\vec{k}_2}})_s=-e^{i\vec{k}_1\cdot\vec{x}}\frac{\partial}{\partial z}\frac{\partial\mu}{\partial\epsilon_{\vec{k}_2}}-e^{i\vec{k}_2\cdot\vec{x}}\frac{\partial}{\partial z}\frac{\partial\mu}{\partial\epsilon_{\vec{k}_1}}-e^{i(\vec{k}_1+\vec{k}_2)\cdot\vec{x}}\frac{\partial^2\mu}{\partial z^2} \ , \tag{19}$$

which must be evaluted to zeroth order in ϵ and at $z=0$. From $\mu^{(0)}$ [Eq. (15)] and $\mu^{(1)}$ [Eq. (18)] we find

$$\frac{\partial}{\partial z}\frac{\partial \mu}{\partial \epsilon_{\vec{k}}}=(dk^2+\alpha-q_0)\left[\frac{q_0}{2}+q(k)\right]e^{i\vec{k}\cdot\vec{x}} \tag{20}$$

and

$$\left.\frac{\partial^2\mu}{\partial z^2}\right|_{z=0,\ \epsilon=0}=-q_0^2 \ . \tag{21}$$

The solution of Eq. (11) thus yields

$$\mu^{(2)}=-\frac{1}{2}\sum_{\vec{k}}e^{i\vec{k}\cdot\vec{x}}\sum_{\vec{k}_1}\epsilon_{\vec{k}_1}\epsilon_{\vec{k}-\vec{k}_1}\{q_0^2+[dk^2+\alpha-q_0]q(k_1) +[d(k-k_1)^2+\alpha-q_0]q(|\vec{k}-\vec{k}_1|)\}e^{-q(k)z} \ , \tag{22}$$

i.e., the second-order contribution to μ.

The procedure should now be clear to the reader; the details of the calculation at orders three to five appear in Appendix A. Once the computations have been carried out to this point, it is relatively easy to write the general solution, which reads

$$\mu=-1+e^{-q_0z}+\sum_{\vec{k}}e^{i\vec{k}\cdot\vec{x}-q(k)z}S(\vec{k}) \ , \tag{23}$$

where

$$S(\vec{k})=\sum_{n=1}^{\infty}\frac{1}{n!}\sum_{\substack{\vec{k}_1,\ldots,\vec{k}_n\\ \sum_i\vec{k}_i=\vec{k}}}\epsilon_{\vec{k}_1}\cdots\epsilon_{\vec{k}_n}r_n(\vec{k}_1,\ldots,\vec{k}_n) \ , \tag{24a}$$

with the r's defined recursively as

$$r_1(k)=-(dk^2+\alpha-q_0) \tag{24b}$$

and

$$(-1)^{n+1}r_n(\vec{k}_1,\ldots,\vec{k}_n)=q_0^n+\sum_{i=1}^{n-1}(-1)^i\sum_{\substack{j_1,\ldots,j_i\\ j_1<\cdots<j_i}}\left[q^{n-i}\left(\left|\sum_l k_{j_l}\right|\right)r_i(\vec{k}_{j_1},\ldots,\vec{k}_{j_i}) +d\bmod(n,2)(-1)^{(n+1)/2}(n-2)!!\times\sum_p\left[\sum_i^n\vec{k}_j\right]\cdot\vec{k}_{j_1}\vec{k}_{j_2}\cdot\vec{k}_{j_3}\cdots\vec{k}_{j_{n-1}}\cdot\vec{k}_{j_n}\right] \ , \quad n\geq 2 \ . \tag{24c}$$

In Eq. (24c), mod$(n,2)$ means n mod2 while the sum $\sum_p$ is over all permutations of the $\vec{k}_{j_i}$ that do not leave the summand trivially invariant, e.g., $j_2\leftrightarrow j_3$ is not allowed but $j_2\leftrightarrow j_4$ is.

We must now, as outlined previously, evaluate the growth rate

$$\dot{z}_s=\sum_{\vec{k}}\dot{\epsilon}_{\vec{k}}e^{i\vec{k}\cdot\vec{x}}+V_z \ . \tag{25}$$

To do this, we compute the impurity flux $\vec{j}=-D\vec{\nabla}\delta c=-D\,\Delta C\,\vec{\nabla}\mu$ [where we have taken into account the normalization (3)], and evaluate it *on* the interface $z=z_s$. Finally, we substitute the surface flux thus obtained into the equation for the conservation of matter at the interface. This last equation can be seen to be

$$j_{sz}+j_{sx}\frac{\partial z_s}{\partial x}+j_{sy}\frac{\partial z_s}{\partial y}=\Delta C\,\dot{z}_s \ . \tag{26}$$

We may now identify the coefficients of $e^{i\vec{k}\cdot\vec{x}}$ on both sides of Eq. (26) in order to get an expression for $\dot{\epsilon}_k$. We find

$$\frac{1}{D}\dot{\epsilon}_{\vec{k}}=\sum_{n=1}^{\infty}\sum_{\substack{\vec{k}_1,\ldots,\vec{k}_n \\ \sum_i \vec{k}_i=\vec{k}}}\epsilon_{\vec{k}_1}\cdots\epsilon_{\vec{k}_n} \times\left\{q_0^{n+1}\frac{(-1)^n}{n!}+\sum_{m=0}^{n-1}\frac{(-1)^m}{m!(n-m)!}r_{n-m}(k_1,\ldots,k_{n-m})\times\left[q^{m+1}\left[\left|\sum_{i=1}^{n-m}\vec{k}_i\right|\right]+mq^{m-1}\left[\sum_{i=1}^{n-m}\vec{k}_i\right]\vec{k}_n\cdot\sum_{i=1}^{n-m}\vec{k}_i\right]\right\} . \tag{27}$$

Details of the derivation appear in Appendix A. Equations (27) are the equations of motion which we have to study. They can be put in nondimensional form by introducing $\vec{\kappa}=\vec{k}(d/\alpha)^{1/2}$, $\nu=V_z/\alpha D$, and $\rho=(\alpha d)^{-1/2}$, rescaling $\epsilon_{\vec{k}}=\alpha^{-1}\epsilon_{\vec{k}}$, and using $\alpha^{-2}D^{-1}$ as the unit of time; we then obtain

$$\dot{\epsilon}_{\vec{\kappa}}=f(\{\epsilon\};\nu,\rho;\vec{\kappa}) \ . \tag{28}$$

For easy reference, the detailed expressions for f are given in Appendix B, together with a complete summary of the notation. Several comments are in order about Eqs. (28) and the parameters that enter in them. We note first the form of the linear contributions to these equations. From Eq. (B2) (see Appendix B) we see that the linear approximation is of the form $\dot{\epsilon}_\kappa=\omega_\kappa\epsilon_\kappa+\cdots$ with

$$\omega_\kappa\simeq\rho\kappa\left[-\frac{\nu^2}{\rho\kappa}+\nu-1-\kappa^2\right] \tag{29}$$

(where the approximation $\rho\gg1$ has been made—see below). This particular structure is familiar from other studies of solidification.[28] It is easy to see from Eq. (29) that the reduced velocity ν plays the role of a driving parameter in our problem; that is, there exists a ν_{cr} such that, for $\nu<\nu_{cr}$, $\omega_\kappa<0\forall\kappa$, while for $\nu>\nu_{cr}=O(1)$, one has a range of wave vectors $[\kappa_1,\kappa_2]$ such that for $\kappa_1<\kappa<\kappa_2$, $\omega_\kappa>0$ and the system is thus linearly unstable—see Fig. 3. Of course, the difficult question concerns the effect of the nonlinear terms: We shall consider this problem in Secs. IV and V. Before doing so, let us comment further on Eqs. (28). We remember that it has been derived under the quasistationary assumption [Eq. (2c')]. We may now state under what circumstances the underlying approximation will be valid. We see from (B2) that a disturbance of interface shape with wave number κ relaxes on a time scale on the order of $(\rho\kappa)^{-1}$; on the other hand, the diffusion field in front of the solidification region has a characteristic time scale $1/Dk^2$ which, in our units, becomes $(\rho\kappa)^{-2}$. Thus we shall be justified in using a stationary form of the diffusion equation, provided $\rho\kappa\gg1$. If we assume that κ remains close to the initially unstable $\kappa\simeq\rho^{-1/2}$ we finally obtain the condition $\rho^{1/2}\gg1$. The parameter ρ is typically[28] of the order of 10^2 and the quasistationary approximation is therefore quite acceptable. As a final and very important remark, we note that Eqs. (28) does not derive from a potential; that is, we *cannot* write $\epsilon_{\vec{\kappa}}=-\partial V/\partial\epsilon^*_{\vec{\kappa}}$, where $V=V(\{\epsilon\};\nu,\rho;\vec{\kappa})$ would be the equivalent of a "free energy" for the problem at hand. While existence of such a function affords (in principle) relatively simple answers to questions related to uniqueness of stationary states, dynamics, etc., its absence leaves us with a much more complicated task. At any rate, however, a hypothetical function V would not have helped much in locating the actual stationary solutions of Eqs. (28), which we now proceed to determine.

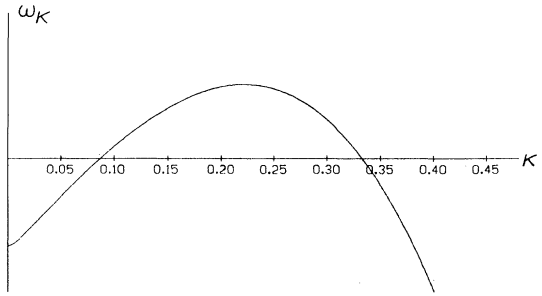

FIG. 3. Linear stability coefficient ω_κ [Eqs. (B2) and (29)] vs the wave number κ, for $\nu=1.15$, $\rho=10^2$. Note that one mode and several harmonics (up to the third) may become simultaneously unstable at such a distance from the threshold ($\nu_{cr}\simeq1.097$, defined as that value of ν for which the first instability occurs).

IV. ONE-DIMENSIONAL STATIONARY SOLUTIONS

The usefulness of a series such as that giving f in Eqs. (28) rests on the fact that the series can be truncated in some consistent fashion and still yield a relatively accurate solution of the problem under consideration. In this section, we use a truncation scheme which seems to provide a good approximation when the stationary solutions of Eqs. (28) are sought. As we shall see, accuracy may require us to keep terms of high order as well as a large number of modes; under these circumstances, one may wonder whether a series expansion is the best procedure to start with. This question may be answered immediately by saying that expanding in this way is the only thing we know how to do. One may be tempted to argue that physical arguments could presumably be adduced in order to describe what happens, say, in the cusps of the cellular interface; this information could then be used somehow in order to simplify the calculations. We believe such a line of reasoning is bound to fail, the fundamental problem being that we are dealing with an equation (2c′) which is *elliptic*. No satisfactory approximation to the solution may be found by considering what happens only in a small neighborhood such as the vicinity of a cusp; rather, it is the whole, global, pattern which must be considered. However, it is very unlikely that "physical" arguments will go beyond spatially *local* balance considerations, etc., and physical reasoning thus appears essentially useless. It is worth noting also that, while some experiments do exhibit very sharp cusps indeed,[26] this is far from always being the case.[37] Thus reliance on the existence of well-defined "mathematical" cusps may be dangerous. We may remark, in this context, that Langer's analysis[18] of the infinite velocity cusp involves, precisely because of the infinite velocity condition, a mutilation of Eq. (2c′), which renders it effectively first order. Since the transition back to large but finite velocity is thus singular, one may wonder whether the infinite velocity analysis is relevant to the actual physics. Finally, it must be emphasized that direct numerical solution of the diffusion equation is difficult and has not led to significant results.[37] All this seems to bring us back to our series expansion, which we now try and use in order to gain information about the stationary configuration of the interface. The results described below have all been obtained numerically.

The structure of the equations, and more specifically the fact that the wave number κ is "conserved" (i.e., the equation for $\dot{\epsilon}_\kappa$ involves only monomials of the form $\epsilon_{\kappa_1}\epsilon_{\kappa_2}\cdots\epsilon_{\kappa_l}$ such that $\sum_{i=1}^{l}\kappa_i=\kappa$) allows us to devise an approximation scheme in the following way. Let us assume that a static one-dimensional solution of Eqs. (28) consists in the superposition of a fundamental frequency κ_0 and of its harmonics; assume furthermore that harmonics 1 to m have an amplitude which is of the order of a [a quantity much smaller than $(\rho\kappa_0)^{-1}$ so that Eq. (B2) makes sense (see below)]. Then, it is easy to see that the stationary values of harmonics $m+1$ to $2m$ must in general be of order a^2, harmonics $2m+1$ to $3m$ will have amplitudes of $O(a^3)$, etc. We are therefore consistent to $O(a^n)$ if we expand formally all equations to this order (taking the above argument into account), while including $n\times m$ modes in the analysis.[38] Of course, the correctness of this scheme must be checked *a posteriori* on the solution $(\epsilon_{\kappa_0},\ldots,\epsilon_{mn\kappa_0})$ thus determined. *In principle,* if the expansion is to be useful at all, we expect that, not too far from threshold, the solution will improve when we increase n and m, at least up to a certain point.

Close to threshold, numerical calculations show that a stationary solution exists for κ_0 anywhere in the range $\omega_{\kappa_0}>0$; the solution is almost sinusoidal and is already well approximated with $m=2,n=3$. Note that the wave numbers κ_0 for which $\omega_{\kappa_0}>0$ are of the correct order of magnitude $\sim 50\ \mu\text{m}^{-1}$. Results of this type have been reported previously by Langer[28] for his "symmetric" model. Langer also observed that, when increasing ν well past threshold, the range of κ_0 over which a stationary solution can be found ceases to coincide with the range $\omega_{\kappa_0}>0$; it seems to us, however, that caution is required here, as we shall try to show below. In addition, Langer discussed the cellular interface relatively far from threshold, where we expect a significant contribution from the harmonics to arise. When doing this, one must try to estimate the precision of the solution. This is difficult to do directly; we shall outline later the procedure we have adopted here.

Let us, for definiteness, take the values $\rho=100$, $\nu=1.15$. This is the case illustrated in Figs. 1 and 3; when $\rho=100$, the threshold is at $\nu\simeq 1.097$. We see that for $\nu=1.15$ (Fig. 3), a given mode and up to two harmonics may become linearly unstable: We may thus say that we are quite far from threshold already. Let us now consider the question of the existence of a stationary solution with a given fundamental wave number κ_0. For example, limiting ourselves to a third-order approximation ($n=3$), we have searched numerically for solutions at $\kappa_0=0.1$ (fairly close to the border of instability). Taking $m=2$, that is, assuming that the fundamental and its second harmonic are of the same order, we find *no* stationary solution. However, with $m=3$, more

modes being thus included in the analysis, we obtain numerically a very reasonable solution, whose appearance still matches quite well with the plots exhibited by Langer.[28] Clearly, this phenomenon is a warning that one should be very careful and not jump hastily to conclusions about the existence or inexistence of solutions at a particular κ_0, as well as about the appearance of "branches" of solutions in a κ_0-amplitude diagram: these conclusions might be spurious and a mere result of the approximations involved.[39] The influence of n—the order of approximation—on all this is not systematic: Increasing n may restore a solution or, alternatively, destroy what was apparently a solution. It is clear that we are dealing here with an expansion which, as was to be expected, is rather badly behaved. In what follows, we shall consider only values of κ_0 for which there exists a stationary solution for several—if not all—values of m and n that we have tested; we shall later on have something to say about the general location of these κ_0's. Assuming such a case, we can then get rather easily a rough idea of the precision of the putative solution by observing the "spread" as the parameters m and n are varied. Unfortunately, simple theoretical or semitheoretical estimates for an upper bound of the error are too large to be of practical use. It is of interest, however, to derive a "lower" bound for the error, which, as we shall see, has the advantage to give us a clear limit as to how far the expansion can possibly be pushed in a favorable case. We therefore estimate the order of magnitude of those terms in the equations of motion which we are neglecting when using a given value of m and n. From Eq. (B2) it is not difficult to see that, if ϵ_{κ_0} is $O(a)$, then contributions of order n to $f_{i\kappa_0}(\{\epsilon\})$ [with $lm+1\leq i\leq(l+1)m$] grow at least like $(\rho\kappa_0)^{n-l}a^n$. This we can take as a rough indication of the minimal error $\delta f_{i\kappa_0}$ on the value of $f_{i\kappa_0}$ when working to order n (barring accidental cancellations). Now since $\epsilon_{i\kappa_0}=O(a^{l+1})$, one can write $0=f_{i\kappa_0}=\omega_{i\kappa_0}\epsilon_{i\kappa_0}+O(\omega_{i\kappa_0}a^{l+1})+\delta f_{i\kappa_0}$, where ω_κ is given by (29); it is thus certainly reasonable to expect $\omega_{i\kappa_0}\delta\epsilon_{i\kappa_0}\simeq\delta f_{i\kappa_0}$, and therefore, the relative error $\delta\epsilon_{i\kappa_0}/\epsilon_{i\kappa_0}>(\rho\kappa_0 a)^{n-l-1}$, assuming that $\omega_{i\kappa_0}=O(\rho\kappa_0)$ (presumably, our formula remains valid as an estimate even when $\omega_{i\kappa_0}$ is $\ll\rho\kappa_0$, as is the case when $i\kappa_0$ is close to the edge of the band of unstable states). Clearly, we thus have to take $l<n-1$, which limits the number of useful modes, the m modes of order a^n being almost certainly meaningless, and check that $\rho\kappa_0 a$ is not too close to 1.

Minimum error estimates obtained in this way check nicely with the spread of amplitude values that one gets when varying n and m, at least in the favorable cases which we consider here. Thus when taking $\kappa_0=0.14$ ($\nu=1.15$, $\rho=100$) we find $a\simeq 3.510^{-2}$, and therefore, $\rho\kappa_0 a\simeq 0.5$; with $n=3$ this yields a maximum precision, for the largest amplitudes, of $\pm 25\%$, while $n=4$ gives $\pm 13\%$. The variations of ϵ_{κ_0} with n are quite consistent with the above lower bounds; in the absence of a meaningful upper bound for the error, these variations are of course the ultimate test of the quality of our approximation. In order for the whole hierarchy of orders of magnitude to hold, however, it becomes necessary, when increasing n, to increase also m, as the higher harmonics tend to grow in importance; this makes for very lengthy calculations when ν gets far from threshold, and $n=5$, say: Thus fifth-order calculations have been carried out only relatively close to threshold, where the results of an $n=5$ computation simply confirm the validity of the $n=3$ or 4 approximations. As an example of numerical results further from threshold, the solution when $n=4$, $m=3$ is, for the case described previously[40] (see Figs. 1 and 3): $\epsilon_1=0.39\times 10^{-1}$, $\epsilon_2=-0.80\times 10^{-2}$, $\epsilon_3=0.25\times 10^{-2}$, $\epsilon_4=-0.15\times 10^{-2}$, $\epsilon_5=0.15\times 10^{-2}$, $\epsilon_6=-0.81\times 10^{-3}$, $\epsilon_7=0.3\times 10^{-3}$, $\epsilon_8=-0.5\times 10^{-4}$, and $\epsilon_9=0.7\times 10^{-5}$, while $\rho\kappa_0 a=0.54$. In Fig. 1, the $n=3$, $m=3$ solution is also represented; when these results are compared with experiment,[26,37] the improvement brought about by the inclusion of high-order terms is quite apparent. Certainly, the effect of those terms goes in the right direction. The striking qualitative change is brought about by the much larger amplitudes of the higher harmonics, which are now determined with better precision. Unfortunately, with $n=5$, consistency of the expansion could not be ensured without a prohibitively large number of modes being needed. This was manifested, in particular, by the appearance of numerous spurious solutions. These can be detected as such because none is sign alternating: this seems to be the hallmark of the well-behaved solutions (see above). It is clear that our results are only a first step in the study of an extraordinarily complicated nonlinear situation; further analysis of the structure of the equations of motion may prove helpful, although the author must confess that he does not know at present how to proceed with such an analysis. Maybe some asymptotic information at large n could be extracted from the series, but their complicated form will render this extremely difficult.

We have mentioned before that a relatively well-defined solution exists only in a certain range of κ_0; two interesting questions then arise: (1) what are the limits of this range, and (2) what—if anything—determines the actual κ_0 observed, which seems quite

sharply defined experimentally. As for question (1), we shall limit ourselves to two general considerations. Firstly, the numerical problems we were alluding to (sensitivity to m and n, etc.)—which may or may not be indicative of actual physical phenomena—arise mainly close to the small-κ_0 limit of the linear instability range; what happens physically is that when κ_0 is small, the harmonics tend to be themselves more unstable; the system is then apparently unable to "quench" these sufficiently. If we attempt a numerical solution with $(\epsilon_{\kappa_0},\epsilon_{2\kappa_0},\epsilon_{3\kappa_0},\epsilon_{4\kappa_0})$, say, we may thus end up with a stationary solution like $(0,\epsilon^s_{2\kappa_0},0,\epsilon^s_{4\kappa_0})$, i.e., the fundamental has become $2\kappa_0$. Interestingly, the "well-behaved" solutions with the lowest possible κ_0 are also those which seem to have the more developed cusps. Thus the numerical instability at low κ_0 appears to be connected with the physical phenomena of cusp "sharpening." This conclusion agrees also with the general trend we have observed, that increasing m may often "reveal" a stationary solution at a value of κ_0 where none was found previously. The second general remark one may make is that the range of well-behaved solutions extends further, at *large* κ_0, than the linear stability curve would suggest. This is in agreement with observations first made by Langer.[28] Behavior close to the large κ_0 limit is generally much smoother and stable than at the other end.

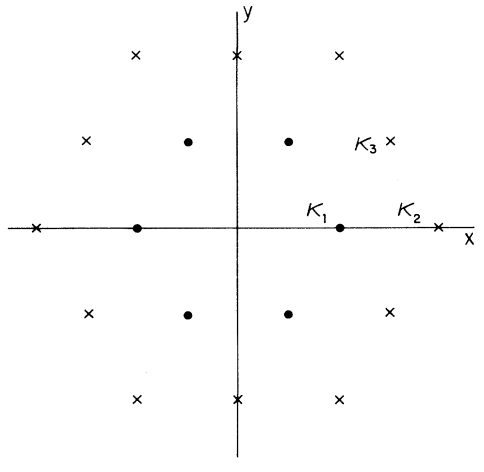

FIG. 4. Fourier modes included in our analysis of two-dimensional solidification patterns (see text and Fig. 2). Symmetry leaves us with three independent amplitudes, for $\kappa_1=(\kappa,0)$, for $\kappa_2=(2\kappa,0)$, and for $\kappa_3=\frac{1}{2}(3\kappa,\sqrt{3}\kappa)$. The amplitude for the $\kappa_0=(0,0)$ mode is zero within our approximations.

As for the second question—what determines κ_0—we can see three possibilities[41]; (a) κ_0 is not actually determined—this possibility cannot be ruled out completely; (b) κ_0 is ultimately fixed by the high n and m terms of Eqs. (28)—this, however, is going to be extremely hard to establish, if our experience is any indication; and (c) the key to selection lies not in the stationary solutions themselves but in the dynamics of the system of equations (28). In a planned future publication[15,42] we shall present the results of dynamic simulations of Eqs. (28); suffice it to say here that, when a Gaussian white-noise source is added to the right-hand side of Eqs. (28), the system exhibits a definite tendency to settle in a well-determined κ_0 state. It is fascinating—and somewhat puzzling—to note that this "selected" κ_0 state seems to lie close to the low κ_0 limit of well-behaved stationary solutions, in other words, the selected κ_0 is one of those associated with the sharpest possible cusps. At the present stage of our investigation, we can only present this observation as a possible—and tantalizing—clue. Let us note finally that in our Fig. (1), we have chosen the value of κ_0 very close to what appears to be the selected κ_0 in that case.

V. TWO-DIMENSIONAL STATIONARY SOLUTIONS

We now turn our attention to the nature of the two-dimensional stationary solutions. Here, we shall not dwell on matters of precision and large distances from threshold; rather, we shall limit ourselves to what happens fairly close to the critical velocity, when a third-order approximation with very few modes included is all that is needed to get a qualitative idea of the appearance of the interface. Part of our results for such a regime are summarized in Fig. 2. We have chosen $\rho=100$ again, and $v=1.105$; the modes that enter in our calculations are represented in κ space in Fig. 4. The first type of solution (not represented in the figure) is of course that where the only modes with nonzero amplitudes are κ_1 and κ_2—these solutions are basically identical to our one-dimensional ones, but now extending as "stripes" in the y direction. Such patterns of rectilinear "grooves" are seen experimentally.[25] The other interesting patterns that are observed[25] all exhibit an approximate sixfold symmetry; it is thus convenient to choose fundamental modes with the same hexagonal degeneracy. Basically, there are four independent modes, $\kappa_0=(0,0)$, $\kappa_1=(0.15,0)$, $\kappa_2=(0.30,0)$, and $\kappa_3=(0.225,0.13)$. We assume that $\epsilon_{\kappa_1}=O(a)$, while ϵ_{κ_2} and $\epsilon_{\kappa_3}=O(a^2)$, and expand to $O(a^3)$. In fact, it turns out that within this approximation, $\epsilon_{\kappa_0}=0$. We find two basic types of station-

ary sixfold-symmetric patterns; they are represented in Figs. 2(a) and 2(b) as contour plots of the surface. One type of pattern corresponds to a triangular "lattice" of "pits"; the other is best described as a honeycomb lattice of grooves. The H in Fig. 2(b) corresponds to the "higher" point on the interface (the hottest one), while the L coincides with the meeting point of three grooves. It is gratifying that these two interface configurations have both been observed in metallurgical systems.[25] It is to our knowledge, the first time that they are analyzed theoretically. Many fascinating questions remain to be studied now that we begin to understand the basic patterns. Foremost is the problem of the relative stability of the three pattern types, stripes, pits, and honeycomb; for instance, do boundary conditions influence this relative stability? What is the effect of noise? How does wave number selection enter here, etc.? Dimensional dependence in far from equilibrium systems is a problem of considerable interest about which we do not yet know much. We hope the results we have presented in this section may open the way for more work along that direction.

VI. REMARKS AND CONCLUSIONS

It is unfortunate—but apparently true—that the only way in which the difficult problem of directional solidification can be studied theoretically is through the solution of the basic equations. This in itself is not an easy task, as may be seen from the length of the calculations involved. Yet it must be stressed that we have used what is probably the most convenient method ever devised to deal[36] with the differential problem at hand. This, however, only allowed us to establish the (autonomous) equations of motion of the system; their stationary solutions are themselves difficult to extract, and a way to systematically evaluate the errors involved is clearly missing. The situation is thus far from being completely satisfactory. In spite of these drawbacks, the expansion technique used in this paper is still the only practicable approach, and our results demonstrate, we believe, its great interest. When pushed to orders four or five, the expansion yields one-dimensional interface profiles that agree fairly well, in their overall features, with what is seen experimentally, while even an expansion to third order is sufficient to reproduce the general aspect of two-dimensional solidification fronts. There are presumably various different ways than the one described here, which would allow us to obtain other useful information out of the equations of motion (28); we hope to come back to this question in the future.

As explained in Secs. IV and V, an outstanding problem is the question of wave-number selection, which occurs here in the same way it shows up in other nonequilibrium systems. In a planned future publication,[15,42] we shall study this in more detail: we have carried out dynamical simulations of the one-dimensional solidification front, and these calculations strongly suggest that, when subjected to Gaussian white noise, the interface selects a particular wave number out of the range of available states.

A final word of caution should indicate to the reader the sort of complication that may arise when analyzing this type of problem. We have assumed throughout that ΔC, the difference in impurity concentration on the two sides of the interface, is independent of the temperature. Although this may appear as a rather innocuous approximation, it is worth noting that reinstating a temperature-dependent miscibility gap ΔC leads to results that are drastically different from those described here. We have checked the equations of motion up to third-order terms in this case, and have been unable to find any stationary solutions for a wide range of parameter values. This result is actually in agreement with Ref. 20, where no static solutions satisfying the quasistationary approximation—assumed here—were found close to threshold. We should thus be warned that in such a strongly nonlinear situation as the one we have tried to analyze, part of the truth may be no truth at all.

ACKNOWLEDGMENTS

We should like to thank Professor B. I. Halperin and Professor P. C. Martin for useful discussions, and are grateful to the Ch. Weizmann Fund for a post-doctoral fellowship. Partial support for this work was provided by the National Science Foundation under Grant No. DMR-82-07431.

APPENDIX A

In this appendix, we describe some of the details in the explicit calculation of the third- to fifth-order terms of the series (23) for μ. We also derive (27) from (23).

In order to evaluate the third-order terms of (24), we need to know $\partial^{(3)} \equiv \partial^3(\mu_s)/\partial\epsilon_{\vec{k}_1}\partial\epsilon_{\vec{k}_2}\partial\epsilon_{\vec{k}_3} \mid_{\epsilon=0}$; from (4) and (14),

$$\partial^{(3)} = d e^{i(\vec{k}_1+\vec{k}_2+\vec{k}_3)\cdot\vec{x}} (\vec{k}_1+\vec{k}_2+\vec{k}_3)\cdot[\vec{k}_1(\vec{k}_2\cdot\vec{k}_3)+\vec{k}_2(\vec{k}_1\cdot\vec{k}_3)+\vec{k}_3(\vec{k}_1\cdot\vec{k}_2)] \ , \tag{A1}$$

where from now on we drop the vector signs. The derivative which corresponds to the correct boundary condition for the problem $D\nabla^2\mu_{\epsilon\epsilon\epsilon}+V_z\partial\mu_{\epsilon\epsilon\epsilon}/\partial z$ is, however, $\Delta^{(3)}_{123}=\partial^3\mu/\partial\epsilon_{k_1}\partial\epsilon_{k_2}\partial\epsilon_{k_3}\,|_{\epsilon=0,\,z=0}$, that is

$$\Delta^{(3)}_{123}=\left[\partial^{(3)}-\sum_{l,m,n}\frac{e^{ik_lx}}{2}\frac{\partial^2}{\partial\epsilon_{k_m}\partial\epsilon_{k_n}}\frac{\partial\mu}{\partial z}+\frac{e^{i(k_l+k_m)x}}{2}\frac{\partial}{\partial\epsilon_{k_n}}\frac{\partial^2\mu}{\partial z^2}-e^{i(k_l+k_m+k_n)x}\frac{\partial^3\mu}{\partial z^3}\right]_{z=0,\,\epsilon=0}, \tag{A2}$$

where $\{l,m,n\}=\{1,2,3\}$ and the sum is over permutations. Remembering (24b) and taking into account the form of the solution at lower orders, we have

$$\begin{aligned}\Delta^{(3)}_{123}=e^{ikx}\{d\vec{k}_3\cdot[\vec{k}_2(\vec{k}\cdot\vec{k}_1)+k_1(\vec{k}\cdot\vec{k}_2)+k(\vec{k}_1\cdot\vec{k}_2)]+q_0^3+q^2(k_1)r_1(k_1)+q^2(k_2)r_1(k_2)+q^2(k_3)r_1(k_3)\\ -q(k_2+k_3)[q_0^2+r_1(k_2)q(k_2)+r_1(k_3)q(k_3)]\\ -q(k_1+k_2)[q_0^2+r_1(k_1)q(k_1)+r_1(k_2)q(k_2)]\\ -q(k_1+k_3)[q_0^2+r_1(k_1)q(k_1)+r_1(k_3)q(k_3)]\}\\ =r_3(k_1,k_2,k_3)e^{ikx}\ ,\end{aligned} \tag{A3}$$

with $q(k)$ defined after Eq. (17), r_i in Eqs. (24b) and (24c), and $k=k_1+k_2+k_3$. Finally, the third-order contribution to μ is

$$\mu^{(3)}=\tfrac{1}{6}\sum_k e^{ikx-q(k)z}\sum_{k_1k_2}\epsilon_{k_1}\epsilon_{k_2}\epsilon_{k-k_1-k_2}r_3(k_1,k_2,k-k_1-k_2)\ , \tag{A4}$$

obtained by solving the equation for $\mu_{\epsilon\epsilon\epsilon}$ with boundary conditions given by (A3). We proceed to fourth order by noting that $\partial^{(4)}=0$, and thus

$$\begin{aligned}\Delta^{(4)}_{1234}=-\sum_{lmnp}\frac{e^{ik_lx}}{6}\frac{\partial^3}{\partial\epsilon_{k_m}\partial\epsilon_{k_n}\partial\epsilon_{k_p}}\frac{\partial\mu}{\partial z}+\frac{e^{i(k_l+k_m)x}}{4}\frac{\partial^2}{\partial\epsilon_{k_n}\partial\epsilon_{k_p}}\frac{\partial^2\mu}{\partial z^2}\\ +\frac{e^{i(k_l+k_m+k_n)x}}{6}\frac{\partial}{\partial\epsilon_{k_p}}\frac{\partial^3\mu}{\partial z^3}-e^{i(k_1+k_2+k_3+k_4)x}\frac{\partial^4\mu}{\partial z^4}\end{aligned} \tag{A5}$$

evaluated at $z=0$, $\epsilon=0$, where again $\{l,m,n,p\}=\{1,2,3,4\}$ and we sum over permutations; carrying out the derivatives yields

$$\begin{aligned}\Delta^{(4)}_{1234}=e^{ikx}[-q_0^4-q^3(k_1)r_1(k_1)-q^3(k_2)r_1(k_2)-q^3(k_3)r_1(k_3)-q^3(k_4)r_1(k_4)\\ +q^2(k_1+k_2)r_2(k_1k_2)+q^2(k_1+k_3)r_2(k_1k_3)+q^2(k_1+k_4)r_2(k_1k_4)+q^2(k_2+k_4)r_2(k_2k_4)\\ +q^2(k_2+k_3)r_2(k_2k_3)+q^2(k_3+k_4)r_2(k_3k_4)\\ +q(k_1+k_2+k_3)r_3(k_1k_2k_3)+q(k_1+k_2+k_4)r_3(k_1k_2k_4)\\ +q(k_1+k_3+k_4)r_3(k_1k_3k_4)+q(k_2+k_3+k_4)r_3(k_2k_3k_4)]\\ =r_4(k_1k_2k_3k_4)e^{ikx}\ ,\end{aligned} \tag{A6}$$

which provides us with the boundary conditions that are to supplement the differential equation for $\mu_{\epsilon_1\epsilon_2\epsilon_3\epsilon_4}$. Thus

$$\mu^{(4)}=\tfrac{1}{24}\sum_k e^{ikx-q(k)z}\sum_{k_1,k_2,k_3}\epsilon_{k_1}\epsilon_{k_2}\epsilon_{k_3}\epsilon_{k-k_1-k_2-k_3}r_4(k_1k_2k_3\,k-k_1-k_2-k_3)\ . \tag{A7}$$

We shall not exhibit this much detail in computing the fifth-order contributions; the interesting new term comes from $\partial^{(5)}$, which is nonzero. $\partial^{(5)}$ is given essentially as the fifth derivative of the fifth-order term in the sum (14). A straightforward but tedious calculation shows this to be

$$\partial^{(5)}=-3d\,e^{i(k_1+k_2+k_3+k_4+k_5)x}\sum_{\{1((23)(45))\}}(\vec{k}_1+\vec{k}_2+\vec{k}_3+\vec{k}_4+\vec{k}_5)\cdot\vec{k}_1\vec{k}_2\cdot\vec{k}_3\vec{k}_4\cdot\vec{k}_5\ , \tag{A8}$$

where the sum is over permutations in which elements or group of elements within parentheses are identified. (Thus 12345 and 14532 count as *one* permutation.) It is now "easy" to find r_5, which is given by (24) with $n=5$. We thus see that formula (24) correctly embodies the pattern which develops in the calculation of the solution, $\mu(x,y,z)$ [Eq. (23)]. Once this has been obtained, we must evaluate the growth rates, i.e., $\dot{\epsilon}_k$. These are the Fourier coefficients of $\dot{z}_s - V_z = \sum \dot{\epsilon}_k e^{i\vec{k}\cdot\vec{x}}$ (where V_z is the imposed velocity). Using Fick's equation giving the flux $\vec{j} = -D\,\Delta C\,\vec{\nabla}\mu$, the balance condition at the interface, Eq. (26), becomes

$$-\frac{\partial\mu}{\partial z}-\frac{\partial\mu}{\partial x}\frac{\partial z_s}{\partial x}-\frac{\partial\mu}{\partial y}\frac{\partial z_s}{\partial y}=\frac{1}{D}\sum_k \dot{\epsilon}_k e^{i\vec{k}\cdot\vec{x}}+q_0\ ; \tag{A9}$$

the components of the gradient can be deduced from the solution Eq. (23), while

$$\left[\frac{\partial z_s}{\partial x},\frac{\partial z_s}{\partial y}\right]=\sum_k ik\epsilon_k e^{ikx}\ .$$

Substituting into (A9) yields

$$\frac{1}{D}\sum_k \dot{\epsilon}_k e^{ikx}+q_0=\sum_k e^{ikx}\left[\sigma(k)q(k)-\sum_{k'}\vec{k}'\cdot(\vec{k}-\vec{k}')\epsilon_{k-k'}\sigma(k')\right.$$
$$\left.+\sum_{n=1}^{\infty}\frac{(-1)^n}{n!}\left[q_0^{n+1}\sigma_n(k)+\sum_{k'}\sigma(k')[q^{n+1}(k')\sigma_n(k-k')\right.\right.$$
$$\left.\left.-q^n(k')\sum_{k''}\vec{k}'\cdot(\vec{k}''-\vec{k}')\epsilon_{k''-k'}\sigma_n(k-k'')]\right]\right] \tag{A10a}$$

with

$$\sigma_n(k)=\frac{(-1)^n}{n!}\sum_{k_1,\ldots,k_n}\epsilon_{k_1}\cdots\epsilon_{k_n}$$

($n>0$ and sum over $\sum_i k_i=k$), while

$$\sigma(k)=\sum_{n=1}^{\infty}\frac{1}{n!}\sum_{k_1,\ldots,k_n}\epsilon_{k_1}\cdots\epsilon_{k_n}r_n(k_1,\ldots,k_n)\ . \tag{A10b}$$

Identifying the coefficients of e^{ikx} in (A10a) yields directly the equations of motion (27). In Appendix B, we exhibit these equations in nondimensional form.

APPENDIX B

For easy reference, we display in this short appendix the equations of motion (28), in dimensionless variables. With the coordinate z_s of the interface given by

$$z_s=\sum\epsilon_{\vec{k}}e^{i\vec{k}\cdot\vec{x}}\ , \tag{B1}$$

we write $\vec{\kappa}=\vec{k}(d/\alpha)^{1/2}$, $v=V_z/\alpha D$, and $\rho=(\alpha d)^{-1/2}$; take furthermore $\epsilon_k\to\alpha^{-1}\epsilon_\kappa$ and $t\to t\alpha^{-2}D^{-1}$, then

$$\frac{d\epsilon_\kappa}{dt}=\sum_{n=1}^{\infty}\sum_{\substack{\kappa_1,\ldots,\kappa_n\\ \sum_i\kappa_i=\kappa}}\epsilon_{\kappa_1}\cdots\epsilon_{\kappa_n}\left[v^{n+1}\frac{(-1)^n}{n!}+\sum_{m=0}^{n-1}\frac{(-1)^m}{m!(n-m)!}R_{n-m}(\kappa_1,\ldots,\kappa_{n-m})\right.$$
$$\left.\times[Q^{m+1}(S_{n-m})+m\rho^2Q^{m-1}(S_{n-m})\vec{\kappa}_n\cdot\vec{S}_{n-m}]\right], \tag{B2}$$

where $R_1(\kappa)=v-1-\kappa^2$, R_n are defined recursively:

$$R_n(\kappa_1,\ldots,\kappa_n)=(-1)^{n+1}\left[\nu^n+\sum_{i=1}^{n-1}(-1)^i\sum_{\substack{j_1,\ldots,j_i\\ j_1<\cdots<j_i}}Q^{n-i}(S'_{j_i})R_i(\kappa_{j_1},\ldots,\kappa_{j_i})\right.$$
$$\left.+\mathrm{mod}\,(n,2)(-1)^{(n+1)/2}[(n-2)!!]\rho^{n-1}\sum_n(\kappa)\right], \tag{B3}$$

and

$$Q(\kappa)=\nu/2+(\nu^2/4+\rho^2\kappa^2)^{1/2},\ \vec{S}_n=\sum_{i=1}^{n}\vec{\kappa}_i,\ S'_{j_i}=\sum_{l=1}^{i}\kappa_{j_l},\ \sum_n(\kappa)=\vec{S}_n\cdot\sum\kappa_{j_1}((\vec{\kappa}_{j_2}\cdot\vec{\kappa}_{j_3})\cdots(\vec{\kappa}_{j_{n-1}}\cdot\vec{\kappa}_{j_n}))\ ,$$

the last sum being on all permutations of 1,2, . . . , n, *except* for interchanges of elements of groups of elements between parentheses.

[1]J. S. Turner, J.-C. Roux, W. D. McCormick, and H. L. Swinney, Phys. Lett. 85A, 9 (1981).

[2]G. Nicolis and I. Prigogine, *Self-Organization in Non-Equilibrium Systems* (Wiley, New York, 1977).

[3]J. Swift and P. C. Hohenberg, Phys. Rev. A 15, 319 (1977).

[4]E. D. Siggia and A. Zippelius, Phys. Rev. Lett. 47, 835 (1981).

[5]Y. Pomeau and P. Manneville, Phys. Lett. 75A, 296 (1980); Y. Pomeau and S. Zaleski, J. Phys. (Paris) 42, 515 (1981); M. C. Cross, P. G. Daniels, P. C. Hohenberg, and E. D. Siggia, Phys. Rev. Lett. 45, 898 (1980).

[6]F. H. Busse, Rep. Prog. Phys. 41, 1929 (1978).

[7]A. C. Newell and J. A. Whitehead, J. Fluid Mech. 38, 279 (1969).

[8]S. Kogelman and R. C. Di Prima, Phys. Fluids 13, 1 (1970).

[9]R. J. Donnelly, K. W. Schwartz, and P. H. Roberts, Proc. R. Soc. London Ser. A 283, 531 (1965); J. P. Gollub and M. H. Freilich, Phys. Fluids 19, 618 (1976).

[10]E. L. Koschmieder in *Proceedings of the Solvay Conference, Brussels, 1978,* edited by G. Nicolis, G. Dewel, and J. W. Turner (Wiley, New York, 1981), and references therein.

[11]H. Swinney, Prog. Theor. Phys. Suppl. 64, 164 (1978).

[12]D. Walgraef, G. Dewel, and P. Borckmans, Adv. Chem. Phys. 49, 311 (1982).

[13]E. Coutsias and B. A. Huberman, Phys. Rev. B 24, 2592 (1981).

[14]D'Arcy Thompson, *On Growth and Form* (Cambridge University, Cambridge, England, 1917).

[15]M. Kerszberg, Phys. Rev. B 27, 3909 (1983).

[16]J. Kepler, *De Nive Sexangula,* in *Opera Omnia VII,* edited by C. Frisch (Heyder and Zimmer, Frankfurt am Main, 1858–1871), p. 715.

[17]U. Nakaya, *Snow Crystals* (Harvard University, Cambridge, Mass, 1954).

[18]J. S. Langer, Rev. Mod. Phys. 52, 1 (1980), and references therein.

[19]W. W. Mullins and R. F. Sekerka, J. Appl. Phys. 34, 323 (1963); 35, 444 (1964).

[20]D. J. Wollkind and L. A. Segel, Philos. Trans. R. Soc. London 268, 351 (1970).

[21]M. Kerszberg, J. Non-Equil. Thermodyn. 5, 165 (1980).

[22]J. S. Langer, Phys. Rev. Lett. 44, 1023 (1980).

[23]V. Datye and J. S. Langer, Phys. Rev. B 24, 4155 (1981).

[24]J. S. Langer and H. Müller-Krumbhaar, Acta Metall. 26, 1681 (1978); 26, 1689 (1978); 26, 1697 (1978).

[25]See, e.g., J. S. Kirkaldy, in *Non Equilibrium Thermodynamics: Variational Techniques and Stability,* edited by R. Donnelly, R. Herman, and I. Prigogine (University of Chicago, Chicago, 1966).

[26]K. A. Jackson, in *Solidification* (American Society for Metals, Cleveland, 1971).

[27]In Jackson's experiments, the control parameter is in fact not the growth velocity, but rather the impurity concentration. However, no fundamental difference arises from this.

[28]J. S. Langer, Acta Metall. 25, 1121 (1977).

[29]We assume the hot and cold plates removed to infinity.

[30]R. Ghez and J. S. Lew, J. Cryst. Growth 20, 273 (1973).

[31]R. Ghez and G. H. Gilmer, J. Cryst. Growth 21, 93 (1973).

[32]A. G. Cullis, D. T. J. Hurle, H. C. Webber, N. G. Chew, J. M. Poate, P. Baeri, and G. Foti, Appl. Phys. Lett. 38, 642 (1981).

[33]See, e.g., L. D. Landau and E. M. Lifschitz, *Statistical Physics,* 2nd ed. (Pergamon, London, 1958), p. 460.

[34]C. E. Weatherburn, *Differential Geometry of Three Dimensions* (Cambridge University Press, Cambridge, England, 1927).

[35]W. K. Burton, N. Cabrera, and F. C. Franck, Trans. R. Soc. A 243, 299 (1951).

[36]D. D. Joseph and R. L. Fosdick, Arch. Ration. Mech. Anal. 49, 321 (1973); see also D. D. Joseph in *Stability of Fluid Motions,* Vols. 27 and 28 of *Springer Tracts in Natural Philosophy* (Springer, Berlin, 1976), or I. Stakgold, *Green's Functions and Boundary Value Problems* (Wiley, New York, 1979).

[37]S. R. Coriell (private communication).

[38]As we shall show, only the first $(n-1)m$ of these modes can be determined with any precision—and the m last modes may thus be ignored altogether.

[39]Note that even the direct numerical solution of a discretized version of Eq. (2c') is still subject to this problem, since a spatial grid of *any* kind implies a high-$\vec{k}$ cutoff, and thus the neglect of certain modes.

[40]Note that $\epsilon_{\kappa=0}$ remains identically zero in this model.

[41]We shall ignore here the possibility that lateral boundary conditions may play a role in the selection problem. The structures are so small (50 μm) compared to apparatus size, that the effect of boundary walls reaches the center of the system only over experimentally inaccessible time scales. Eutectic solidification affords an excellent experimental illustration of the apparent irrelevance of lateral boundaries for wave number selection in large systems. See, e.g., D. P. Woodruff, *The Solid Liquid Interface* (Cambridge University Press, Cambridge, England, 1973).

[42]M. Kerszberg (unpublished).